Functional Prostate MR Including Dynamic Contrast-Enhanced T1-Weighted Imaging at 1.5 Tesla Without Endorectal Coil.

First Clinical Experiences with a Study Protocol at Multi-Imagem, Brazil

Leonardo Kayat Bittencourt, M.D.; Thomas Doring, MSc; Marcio Bernardes, RT; Emerson Gasparetto, M.D., Ph.D.; Romeu Cortês Domingues, M.D.

CDPI Clínica de Diagnóstico Por Imagem, Multi-Imagem, UFRJ - Federal University of Rio de Janeiro, Rio de Janeiro, Brazil

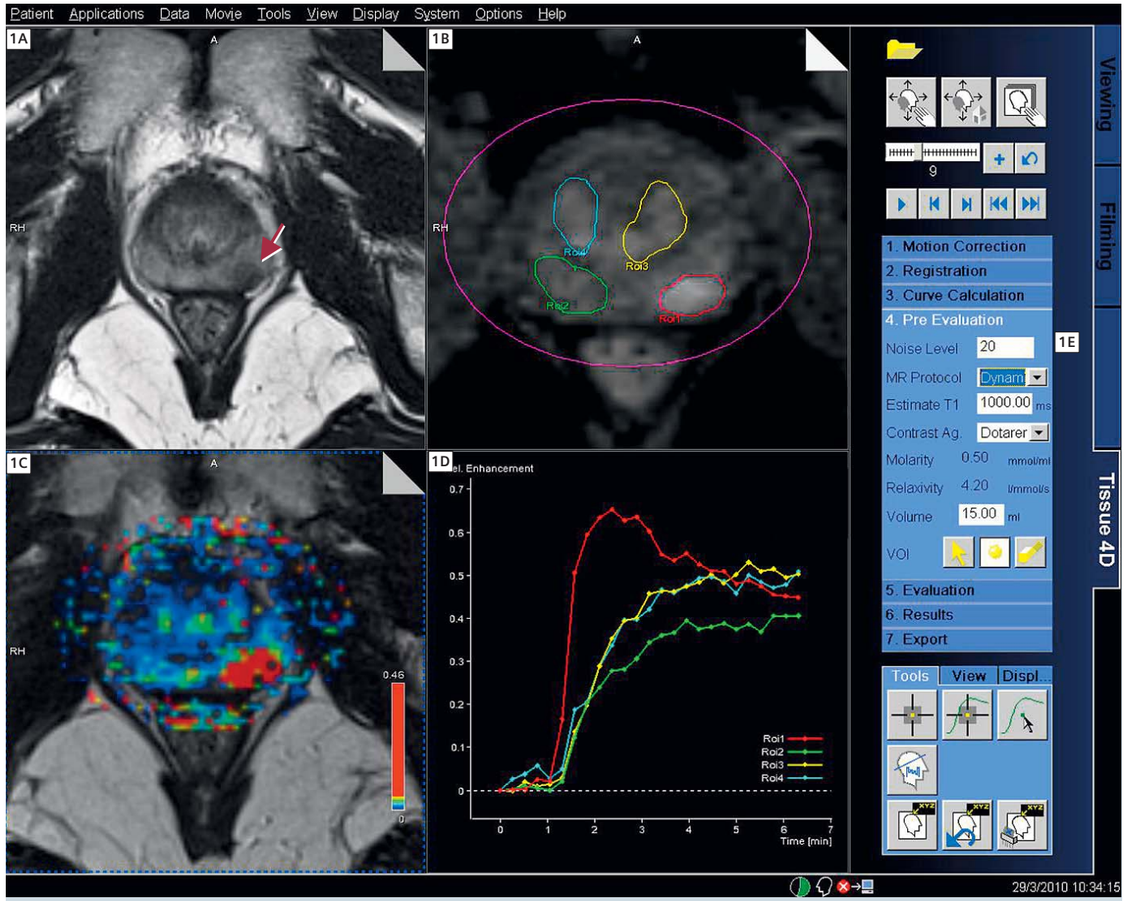

1 *syngo* Tissue 4D screen capture, depicting its four panels, with anatomical (T1w or T2w) images in **1A**, (subtracted) image of dynamic data set in **1B**, parametric maps (K_{trans}, Kep, Ve, iAUC) overlaid on anatomy in **1C**, and relative enhancement curves in **1D**. Note that the suspicious T2w hypointense area in **1A** (arrowhead) corresponds to the red ROI in **1B**, the focally increased K_{trans} area in **1C** and early/intense enhancing curve with washout in **1D**.

Introduction

Reviewing the current literature on prostate MR, most authors rely on the use of 3T scanners that reveal better diagnostic and staging accuracy than the previous studies using older 1.5T and 1.0T machines in the 90's. However, in most countries 1.5T MR scanners are still more widely available than 3T machines. Looking at new developments in coil technology this new generation of 1.5 Tesla superconducting MR scanners potentially provides an acceptable performance on the management of prostate cancer (PCa) patients. Moreover, the continuing improvement of functional sequences, namely diffusion-weighted imaging (DWI) and dynamic contrast enhancement (DCE) T1w imaging and the development of new post-processing tools (i.e., image-fusion and pharmacokinetic maps) could further contribute on the diagnostic and staging accuracy of MRI including 1.5T MR scanners. Based on the literature, multi-modal imaging of the prostate at 1.5 Tesla includes the usage of an endorectal coil. However, in clinical routine the application of such a coil can be restricted by various reasons such as proctitis. However, it should also be taken into account that the procedure of placing an endorectal coil can result in low acceptance of the exam and potentially reduces patient compliance significantly. Therefore it is of high clinical interest to better understand the potential but also the limitations of prostate MRI at 1.5 Tesla without application of an endorectal coil. In this article, we describe in detail our prostate MR protocol and post-processing parameters at 1.5 Tesla without endorectal coil with special focus on DCE T1w imaging, and briefly present the preliminary results, with illustrative cases.

Table 1

Feature	Prostate MR	Histopathology
Unilateral Involvement	3	2
Bilateral Involvement	10	11
Extra-prostatic extension	3	4
Seminal Vesicle extension	1	1
Positive Lymph Nodes	0	0

Materials and methods

This protocol was developed in 2009, as part of an ongoing long-term prostate MR research project. The study was approved by the local Ethics and Research Committee, and all patients signed an informed consent.
Thirteen consecutive patients were submitted to prostate MR examinations, prior to prostatectomy. Patients' age ranged between 51 and 77 years (average 63 years), their PSA levels varying between 3.4 and 42.0 ng/mL (median 8.6 ng/mL). Examinations (table 1) were done on an 18-channel 1.5T scanner (MAGNETOM Avanto, Siemens Healthcare, Erlangen, Germany), with a combination of the 6-channel phased-array surface coil (Body Matrix) combined with up to 6 elements of the integrated spine coil. Prior to the examinations, the patients were given 10 mg of n-methil-scopolamine bromide (Buscopan®, Boehringer Ingelheim, Brazil), in order to attenuate peristalsis. The study protocol consisted of high-resolution T2-weighted turbo spin echo (TSE) sequences in the axial (TR 4750 ms, TE 101 ms, no PAT, FOV (160 x 160) mm^2, matrix (256 x 230) px^2, slice thickness 3 mm, no gap, 3 averages, acquisition time 5:47 min), coronal (TR 3000 ms, TE 101 ms, no PAT, FOV (160 x 160) mm^2, matrix (256 x 230) px^2, slice thickness 3.5 mm, 20% gap, 2 averages, acquisition time 2:15 min) and sagittal (TR 3800 ms, TE 100 ms, no PAT, FOV (170 x 170) mm^2, matrix (320 x 240) px^2, slice thickness 3 mm, 10% gap, 2 averages, acquisition time 3:21 min) planes, high-resolution axial dark fluid T1-weighted sequence (TIRM; TR 2100 ms, TE 20 ms, TI 829.7 ms, PAT factor 2 (*syngo* GRAPPA), FOV (200 x 180) mm^2, matrix (256 x 200) px^2, slice thickness 3 mm, 10% gap, 2 averages, acquisition time 3:09 min), DWI (*syngo* REVEAL) in the axial plane (ep2d_diff; TR 3000 ms, TE 88 ms, b-values 0, 500, 1000 mm/s^2, 3-scan trace, ADC map Inline, noise level set to 0, PAT factor 2 (*syngo* GRAPPA), FOV (200 x 200) mm^2, matrix (150 x 150) px^2, slice thickness 3.5 mm, no gap, 8 averages, acquisition time 2:57 min), thick-slice T2-weighted sequence in the axial plane covering lymph node stages from the renal veins down to the pubic bone (HASTE; TR 700 ms, TE 38 ms, PAT factor 2 (*syngo* GRAPPA), FOV

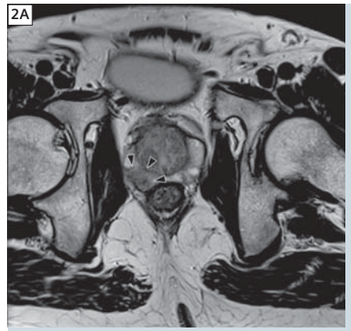

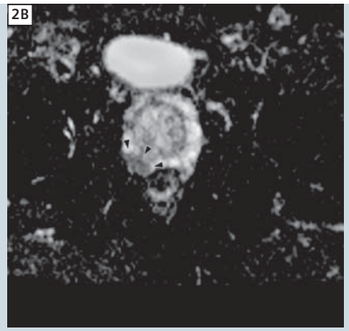

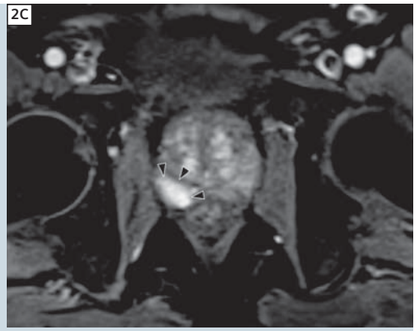

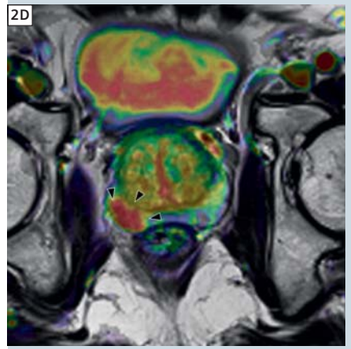

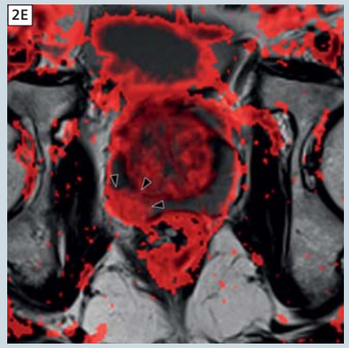

2A–G Prostate cancer with ex-vivo and pathologic correlation.
2A T2-weighted image
2B ADC map
2C Early arterial phase post-gadolinium
2D K_{trans} overlaid on T2w
2E ADC map overlaid on T2w

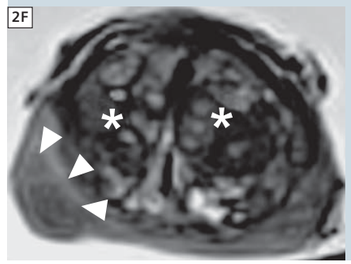

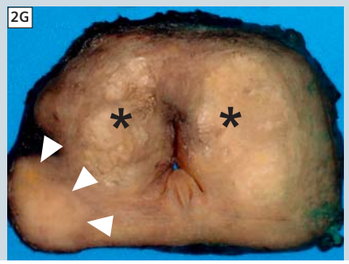

2F Ex-vivo prostatectomy specimen T2w MR
2G Whole-mount processing of a similar section as of MR imaging. The suspicious lesion (arrowheads) on the right middle-third peripheral zone is well depicted in all of the modalities, with good correlation to the pathological specimen.
* = Hyperplasia.

(350 x 317) mm^2, matrix (512 x 440) px^2 (interpolated), slice thickness 5 mm, 100% gap, 1 average, acquisition time 0:30 min), and DCE T1w images acquired with a 3D gradient echo (GRE) sequences (VIBE; TR 4.08 ms, TE 1.43 ms, PAT factor 2 (*syngo* GRAPPA), no fat saturation, FOV (280 x 280) mm^2, matrix (192 x 192) px^2, slice thickness 3 mm, 1 average, 40 measurements, 6.8 seconds per measurement, total acquisition time 4:33 min) (cubital intravenous application of 0.2 mmol/kg of gadolinium-chelate (DOTAREM, Guerbet, Aulnay-sous-Bois, France) on an MR-compatible power injector (Injektron 82 MRT, Medtron, Saarbrücken, Germany) between the second and third measurements). The whole examination took about 30 minutes.
Recently, we also added multi-flip angle volumetric T1w sequences (VIBE, same parameters as above, 1 measurement each, respectively 2°, 5°, 8° and 15° flip angle) prior to contrast injection, in order to estimate the T1 value, so as to enable accurate transfer constant (k_{trans}) calculation on DCE post-processed.
DCE images were post-proccessed using a work-in-progress package of the *syngo* Tissue 4D application. The *syngo* Tissue 4D applications allows pharmacokinetic modeling according to the Tofts-model including parameter calculations, namely transfer constant (k_{trans}), volume constant (Kep), extra-cellular volume of distribution (Ve) and integral area under the curve (iAUC). In addition, parametric color-maps can be generated and fused over MR morphology to allow accurate and fast assessment of the prostate parenchyma, and also to enable accurate measurements of pharmacokinetic parameters on suspected areas (Fig. 1). There is a built-in function to correct for movement between acquisition phases, which we use whenever required. The curve calculation is based on the placement of regions-of-interest (ROIs) (for evaluation of data, four ROIs were evaluated in our study: ROI 1: suspected lesion, ROI 2: contralateral peripheral zone, ROI 3: ipsillateral central gland, ROI 4: contralateral central gland). For calculation of parameters, the software requires input by the user; pre-evaluation parameters used in this study are as follow: noise level: 20, MR protocol: T1 and Dynamic, Contrast agent: Dotarem, volume: variable. The volume-of-interest (VOI) is defined by an elliptical area – drawn by the user – which encompasses the whole prostate volume. The parametric maps are generated from the full VOI, using the Tofts-model. For this, an arterial input function has to be selected; in most of our patients, a "slow" arterial input function has been chosen. K_{trans} and iAUC maps are saved as DICOM series, for further post-processing.
Post-processed images are afterwards overlaid on transverse T2w images, using *syngo* 3D-FUSION® (Siemens Healthcare, Erlangen, Germany), using PET-Rainbow and Descending Red Ramp color look-up tables, respectively for the k_{trans} and the ADC map.
For evaluation of findings within the study setting, one reader (LKB, 5 years of experience, 2 years on prostate MR) evaluated all of the examinations and imaging findings were registered on a dedicated evaluation sheet. Focused on the evaluation of capsular penetration of prostate cancer for planning of radical prostatectomy, suspected lesions were characterized by laterality (left x right x bilateral), presence of local extra-prostatic extension and seminal vesicle involvement. Prostatectomy specimens were submitted to routine histopathological evaluation, except for one, submitted to whole-mount processing.

Results

Prostatectomy showed prostate adenocarcinoma in all 13 cases, with Gleason grades varying between 6 (3+3) and 9 (4+5) (median 6).
In all 13 cases the main tumor focus was correctly identified by MR imaging. The laterality of the lesion was correctly determined by MR in 12 patients (sensitivity: 90%, specificity: 100%), eleven of which

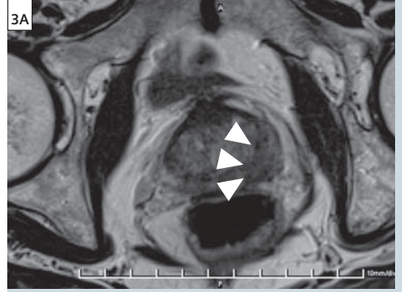

3A–E Extra-prostatic extension.
3A T2w image showing a nodular T2 hypointense area on the left base (arrowheads), focally bulging the capsular contour.

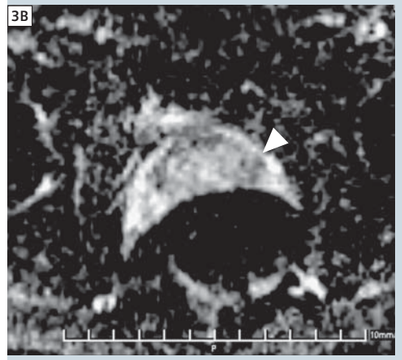

3B On the ADC map, there is restricted diffusion on the same spot, but further anatomical information.

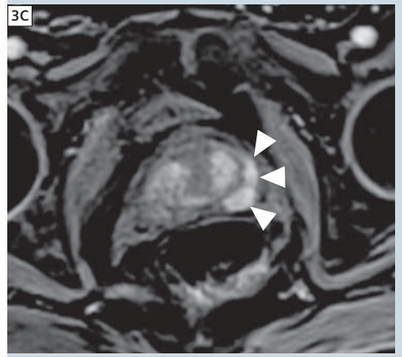

3C Early arterial phase post-gadolinium image, depicting intense and early enhancement on the suspicious area (arrowheads).

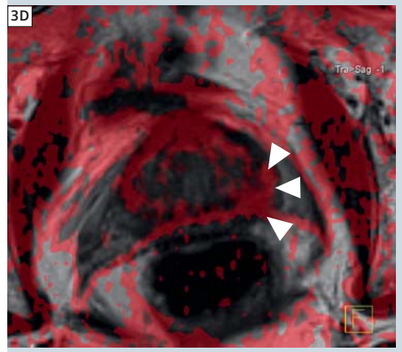

3D ADC map overlaid on T2w image, confirming good correlation with both anatomical and functional findings.

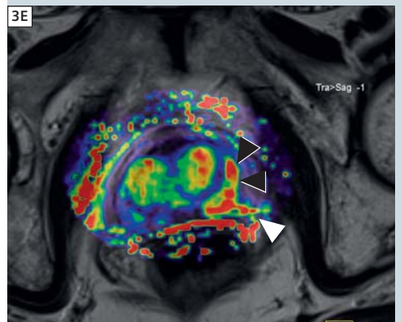

3E K_{trans} map overlaid on T2w image, showing that the focal permeability abnormalities (black arrowheads) extend outside the prostate contour (white arrowhead), strengthening the suspicion for extra-prostatic extension. This was the only sequence that depicted abnormal findings outside of the prostate parenchyma, showing the importance of multimodality imaging on the evaluation of prostate cancer.

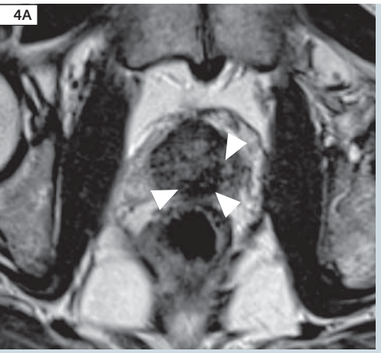

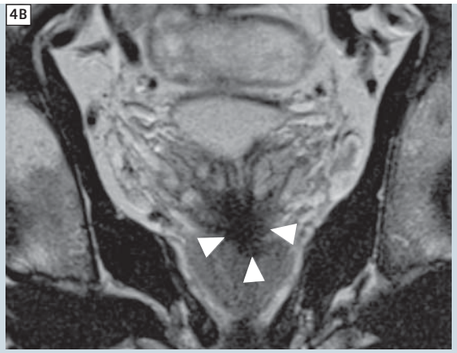

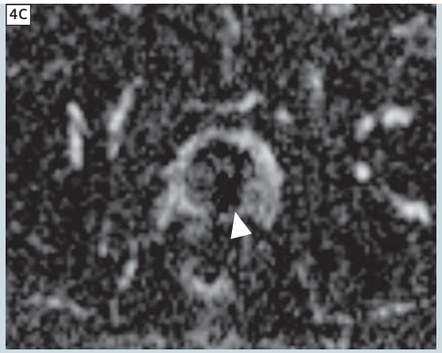

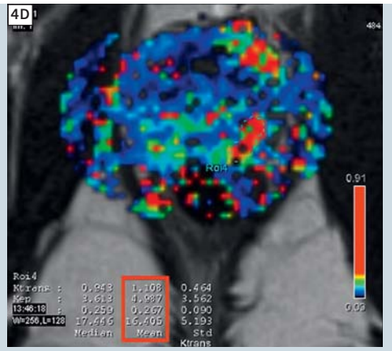

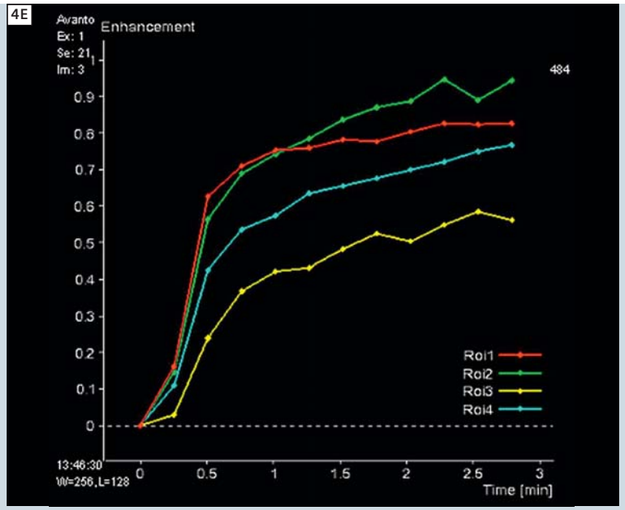

4A–E Seminal vesicle involvement.
4A Axial T2w image, showing a diffusely T2 hypointense prostate parenchyma, which lowers the accuracy for finding focal suspicious areas. There is although an overtly hypointense focus involving the proximal ejaculatory ducts (arrowheads), raising awareness for seminal vesicle extension.

4B Coronal T2w image, nicely showing the suspicious area, with clear involvement of both seminal vesicles.

4C ADC map, showing restricted diffusion on the same area.

4D K_{trans} map overlaid in T2w image, where a focal area of increased permeability (light-blue ROI) is seen, in keeping with the T2 hypointense lesion seen in **4A**, also showing quantitative data (red rectangle).

4E The lesion enhancement curve (red) is the steeper, with tendency to form a plateau rather than to keep on increasing.

had bilateral tumors. There was one false negative, in a patient with bilateral involvement substaged as unilateral tumor by MR.
Four patients had extra-prostatic tumoral extension, three of them being identified by MR imaging (sensitivity: 75%, specificity: 100%).
Only one patient had seminal vesicle tumoral invasion, also seen on MR imaging.
No patient had tumor-positive pelvic lymph nodes, neither was it suspected by MR in any of them.

Discussion

Functional prostate MR imaging, including DWI, DCE, and 3D multi-voxel spectroscopy, is largely turning into the mainstay in prostate cancer detection, staging and follow-up. The results among various institutions bear good to optimal correlation with histopathology, depending on the scanner's field strength (1.5T x 3.0T), the kind of coil employed (surface only x surface + endorectal), and also the gold standard utilized (biopsy x routine histopathology x whole-mount histopathology).
In this context, there's a tendency pointing towards studies on 3T prostate MR, with the combination of surface and endorectal coils, compared with whole-mount histopathology, in order to ally the most recent technology with the highest theoretical spatial resolution achievable. However, this approach creates a potential dilemma for health care providers, public health authorities and general radiology departments, considering that PCa is the most prevalent neoplasm in men, and the availability of 3T scanners worldwide still does not match the demand for diagnosis, staging and follow-up for this condition. Despite the most recent technological advances, an alternative should be pursued for MR imaging of PCa, that allies cost-effectiveness and scanner availability with acceptable diagnostic accuracy, in order to extend the benefits of the technique to the overall population, which is still being managed based on PSA and rectal exam alone.
Also, the endorectal coil (ERC) is another barrier to the acceptance of prostate MR. Although being of undisputedly better performance than surface coil alone on tumor localization, patient refusal due to cultural identity is still a major issue, most notably in Latin and Asian/Arabic countries. It requires specially trained personnel for proper placement, and considerably increases table time, not to mention the deformation produced on the prostate, that compromises radiotherapy planning and follow up studies. Particularly in Brazil, there is also an economical problem, for the ERC, which is disposable and for one use only, is not reimbursed by any of the health insurance companies or the public health system.
Giving those circumstances, and considering that our institutions are localized in a developing country, we initiated a long-term prospective research project aiming to create a prostate MR protocol that is feasible in most of the already worldwide installed 1.5T scanners, without the need of an endorectal coil or specially trained personnel, with optimized table time, and bearing acceptable diagnostic accuracy for relevant staging parameters, to be applied in large populational studies.
We also believe that newer post-processing tools for functional sequences, producing parametric color maps and fusions of functional and anatomic images, may further add to the diagnostic performance and to the communication of results to the referring physicians.
Preliminary results indicate a promising performance of this protocol on presurgical staging of PCa. Further patients will be included, and the upcoming results will be accordingly published.

References

1 Ross R, Harisinghani M. Prostate cancer imaging – what the urologic oncologist needs to know. Radiol Clin North Am 2006; 44:711-722, viii.
2 Somford DM, Futterer JJ, Hambrock T, Barentsz JO. Diffusion and perfusion MR imaging of the prostate. Magn Reson Imaging Clin N Am 2008; 16:685-695, ix.
3 Jung JA, Coakley FV, Vigneron DB, et al. Prostate depiction at endorectal MR spectroscopic imaging: investigation of a standardized evaluation system. Radiology 2004; 233:701-708.
4 Futterer JJ, Heijmink SW, Scheenen TW, et al. Prostate cancer localization with dynamic contrast-enhanced MR imaging and proton MR spectroscopic imaging. Radiology 2006; 241:449-458.
5 Bloch BN, Furman-Haran E, Helbich TH, et al. Prostate cancer: accurate determination of extracapsular extension with high-spatial-resolution dynamic contrast-enhanced and T2-weighted MR imaging – initial results. Radiology 2007; 245:176-185.
6 Weinreb JC, Blume JD, Coakley FV, et al. Prostate cancer: sextant localization at MR imaging and MR spectroscopic imaging before prostatectomy – results of ACRIN prospective multi-institutional clinicopathologic study. Radiology 2009; 251:122-133.
7 Langer DL, van der Kwast TH, Evans AJ, Plotkin A, Trachtenberg J, Wilson BC, Haider MA. Prostate tissue composition and MR measurements: investigating the relationships between ADC, T2, K(trans), v(e), and corresponding histologic features. Radiology. 2010 May;255(2): 485-94.
8 Turkbey B, Pinto PA, Mani H, Bernardo M, Pang Y, McKinney YL, Khurana K, Ravizzini GC, Albert PS, Merino MJ, Choyke PL. Prostate cancer: value of multiparametric MR imaging at 3 T for detection – histopathologic correlation. Radiology. 2010 Apr;255(1):89-99.
9 Groenendaal G, Moman MR, Korporaal JG, van Diest PJ, van Vulpen M, Philippens ME, van der Heide UA. Validation of functional imaging with pathology for tumor delineation in the prostate. Radiother Oncol. 2010 Feb;94(2):145-50.
10 Langer DL, van der Kwast TH, Evans AJ, Trachtenberg J, Wilson BC, Haider MA. Prostate cancer detection with multi-parametric MRI: logistic regression analysis of quantitative T2, diffusion-weighted imaging, and dynamic contrast-enhanced MRI. J Magn Reson Imaging. 2009 Aug;30(2):327-34.
11 Franiel T, Lüdemann L, Rudolph B, Rehbein H, Stephan C, Taupitz M, Beyersdorff D. Prostate MR imaging: tissue characterization with pharmacokinetic volume and blood flow parameters and correlation with histologic parameters. Radiology. 2009 Jul;252(1):101-8.
12 Ren J, Huan Y, Wang H, Ge Y, Chang Y, Yin H, Sun L. Seminal vesicle invasion in prostate cancer: prediction with combined T2-weighted and diffusion-weighted MR imaging. Eur Radiol. 2009 Oct;19(10):2481-6.
13 Fütterer JJ, Barentsz JO, Heijmink SW. Value of 3-T magnetic resonance imaging in local staging of prostate cancer. Top Magn Reson Imaging. 2008 Dec;19(6):285-9.
14 McMahon CJ, Bloch BN, Lenkinski RE, Rofsky NM. Dynamic contrast-enhanced MR imaging in the evaluation of patients with prostate cancer. Magn Reson Imaging Clin N Am. 2009 May;17(2):363-83.

Contact
Thomas Doering
Medical Physicist MRI, MSc
Post-processing Laboratory
CDPI & Multi-imagem
Rio de Janeiro
Brazil
Tel. +55 21 2432 9194
thomas.doring@gmail.com

L. Kayat Bittencourt, M.D.
CDPI & Multi-Imagem
Rio de Janeiro
Brazil
lkayat@gmail.com